This document was prepared in conjunction with work accomplished under Contract No. DE-AC09-96SR18500 with the U.S. Department of Energy.

Electrochemical Studies on the Corrosion of Carbon Steel in Oxalic Acid Cleaning Solutions

B. J. Wiersma and J. I. Mickalonis
Savannah River National Laboratory
Aiken, SC, 29808

ABSTRACT

The Savannah River Site (SRS) will disperse or dissolve precipitated metal oxides as part of radioactive waste tank closure operations. Previously SRS has utilized oxalic acid to accomplish this task. Since the waste tanks are constructed of carbon steel, a significant amount of corrosion may occur. Although the total amount of corrosion may be insignificant for a short contact time, a significant amount of hydrogen may be generated due to the corrosion reaction. Linear polarization resistance and anodic/cathodic polarization tests were performed to investigate the corrosion behavior during the process. The effect of process variables such as temperature, agitation, aeration, sample orientation, light as well as surface finish on the corrosion behavior were evaluated. The results of the tests provided insight into the corrosion mechanism for the iron-oxalic acid system.

Keywords: oxalic acid, carbon steel, radioactive waste tanks, hydrogen, electrochemical testing

INTRODUCTION

Sludge removal will be performed as part of waste tank closure operations. Typically the bulk sludge is removed by simple water slurry and decant operations. Experience has shown that a residual heel remains that cannot be removed by this conventional technique. In the past, SRS has utilized oxalic acid solutions to break down or dissolve the sludge heel so that the removal can be completed. Since the waste tanks and cooling coils are constructed of carbon steel a significant amount of corrosion may occur during cleaning with oxalic acid. Although the total amount of corrosion may be insignificant for a short contact time, a significant amount of hydrogen may be generated due to the corrosion reaction. It has been estimated that given a 100 mpy corrosion rate and no ventilation the lower flammability limit (LFL) will be reached in less than seven days. As a result, costly safety class equipment upgrades might be required for flammability control of the waste tank.

A literature review provided limited information on changes in corrosion rate of carbon steel as the oxalic acid dissolved the sludge. Generally, the corrosion studies focused on coupon tests performed over a specific test period in oxalic acid alone. Thus, it is difficult to determine if the corrosion rate changes with time in a realistic system. Because of the passivation reactions that occur during corrosion of carbon steel in oxalic acid, the tests may give an overestimate of the actual corrosion rate particularly as it applies to a specific process. The review also suggested that cathodic reactions other than hydrogen evolution might be occurring during the corrosion process. Other potential cathodic reactions include oxygen reduction or the reduction of another anion in solution such as nitrate. If it can be shown that either the rate decreases

with time or that these other cathodic reactions predominate, installation of the safety class equipment and controls may not be necessary.

Corrosion is a process that involves electrochemical as well as chemical reactions. The electrochemical reactions differ from the chemical reactions in that an exchange of electrons occurs at the interface between the metal and the solution. In order to maintain a balance of charge, two reactions occur at the surface. The metal dissolution reaction, or anodic reaction, results in the loss of electrons, while the coupled cathodic reaction results in a species gaining electrons. An example of these two reactions is shown in equations 1 and 2, where iron is being oxidized to a ferrous species while hydrogen ions are being reduced producing hydrogen, which is evolved as a gas [1].

$$Fe^{\circ} \longrightarrow Fe^{2+} + 2e^{-} \qquad (1)$$

$$2H^{+} + 2e^{-} \longrightarrow H_2\uparrow \qquad (2)$$

However, if oxygen is present in the system, the cathodic reaction is accelerated by a process known as depolarization. Oxygen reduction occurs by the following reaction:

$$O_2 + 4H^{+} + 4e^{-} \longrightarrow 2H_2O \qquad (3)$$

Given the components present in the sludge, other cathodic reactions are also possible such as the reduction of ferric to ferrous ions or the reduction of nitrate to nitrite.

Ferrous hydroxide ($Fe(OH)_2$) forms as a film on the metal surface and serves as a diffusion barrier layer through which O_2 must diffuse to reach the metal surface. As the ferrous hydroxide is further exposed to oxygen it reacts to oxidize the ferrous iron to ferric iron in the form of ferric oxide (Fe_2O_3) and ferric hydroxide ($Fe(OH)_3$), which are the reddish brown colors normally associated with steel corrosion products.

In an 8 wt.% oxalic acid environment, oxalic acid dissociates into the hydrogen-oxalate (HC_2O_4-) species and hydrogen cation. Recent electrochemical tests [2] indicate that the hydrogen-oxalate species participates in the metal dissolution reaction as shown in Equation (4).

$$2Fe^{\circ} + HC_2O_4^{-} \longrightarrow FeC_2O_4 + Fe^{2+} + H^{+} + 4e^{-} \qquad (4)$$

If hydrogen is the cathodic reaction, the overall corrosion reaction is given by Equation (5):

$$2Fe^{\circ} + HC_2O_4^{-} + 3H^{+} \longrightarrow FeC_2O_4 + Fe^{2+} + 2H_2\uparrow \qquad (5)$$

On the other hand, if oxygen depolarization occurs the overall reaction is given by Equation (6) as:

$$2Fe^{\circ} + HC_2O_4^{-} + 3H^{+} \longrightarrow FeC_2O_4 + Fe^{2+} + 2H_2O \qquad (6)$$

The ferrous species reacts with water again to produce the ferrous hydroxide, which again is further oxidized to the ferric oxide species. In addition to the ferric oxide corrosion products, Equation 6 indicates that the ferrous oxalate ($FeC_2O_4 \cdot 2H_2O$) species forms on the surface. This species has a yellowish-green appearance and serves to passivate the surface as well.

Ferric ion is present in some of the dissolved sludge solutions. The reduction of ferric iron to ferrous iron is another possible cathodic reaction [3]. The cathodic reaction in this case would be:

$$Fe^{3+} + e^{-} \longrightarrow Fe^{2+} \qquad (7)$$

The overall corrosion reaction if ferric iron reduction serves as the cathodic reaction is given by Equation (8) as:

$$Fe^{\circ} + HC_2O_4^- + 2\,Fe^{3+} \longrightarrow FeC_2O_4 + 2\,Fe^{2+} + H^+ \qquad (8)$$

In addition to this electrochemical process, ferrous oxalate can also form by a photochemical process as shown in Equations (9) and (10):

$$Fe^{3+} + 3\,C_2O_4^{2-} = Fe(C_2O_4)_3^{3-} \qquad (9)$$

$$2\,Fe(C_2O_4)_3^{3-} = 2\,FeC_2O_4 + 3\,C_2O_4^{2-} + 2\,CO_2 \qquad (10)$$

The first step is the formation of the anionic, iron (III) trisoxalate complex, $Fe(C_2O_4)_3^{3-}$, which then undergoes photochemical induced decomposition producing ferrous oxalate, oxalate and carbon dioxide. The trisoxalate complex is highly soluble and is recognizable by its lime green color in solution [4]. This anion decomposes photocatalytically over a period of days, depending on the radiation intensity in the visible range. Consequently, ferrous oxalate compound precipitates on the metal surface. Reaction (10) also shows a mechanism by which carbon dioxide evolves during this process.

The purpose of these electrochemical tests was to determine the effect of various process variables (e.g., agitation, temperature, etc) associated with chemical cleaning on the anodic and cathodic reactions. Anodic potentiodynamic polarization tests were performed to study the stability of the ferrous films (oxide and oxalate) that are formed at various environmental conditions. Cathodic potentiodynamic polarization tests were performed to examine which cathodic process was occurring and the impact of these process variables on the rate that it occurs.

EXPERIMENTAL

Materials

Table 1 shows the composition of ASTM A537 Class I steel that was utilized for these tests. The initial surface condition of the coupons was a 600 grit polished finish (See Figure 1a). The polished coupons provide a uniform, reproducible surface finish ideal for studying reactions between the steel and the environment. Previous laboratory studies on the corrosion of carbon steel in oxalic acid have primarily utilized polished coupons [5]. However, the metal surface conditions inside the tank are very different. Steel plates from the foundry, similar to those used to build the waste tanks, typically have an adherent iron oxide film on the surface referred to as mill scale. The presence of this film would be expected to produce a different corrosion response than the polished surface, at least initially. To simulate the mill scale in these tests, coupons were placed in a Thermolyne™ benchtop muffle furnace set at 700 °C for 20 minutes. The result was a uniform oxide that was identified by x-ray diffraction as primarily magnetite (see Figure 1b). Finally, the tank steel has been exposed to caustic supernate for many years. To simulate this exposure, the mill-scale coupons were immersed in supernate for a minimum of 24 hours and then dried. This step left the coupon encrusted with a salt layer similar to the condition of the tank walls.

In addition to the mill-scale finish, two other surface conditions were examined. In humid environments water condenses on the surface of the coupon and general corrosion or pitting of the surface occurs. Depending on the level of contaminants in the vapor space and the temperature, this can vary from light surface rusting to heavy corrosion products. During recent coupon testing in support of chemical cleaning corrosion due to condensation in the vapor space left the coupons covered with iron oxide corrosion products [1]. These iron oxides may result in very different corrosion behavior in the oxalic acid-sludge mixture. Therefore, electrochemical testing on two other surface conditions was performed, i.e., polished coupons that had been exposed to water and mill-scale samples that been exposed to water. In each case the surface of the coupon became covered with iron oxide corrosion products before testing.

Equipment

The tests were conducted in one of two cells as shown in Figure 2. The glass cell was utilized for tests in a lighted environment, while a stainless steel cell was used for tests in a dark environment. Each cell

consisted of four primary features: a) a working electrode, b) a counter electrode, c) a reference electrode, and d) a potentiostat. Each is briefly described below.

The working electrode is the material that is being tested, which in this case are the carbon steel coupons. The coupons were prepared for testing by attaching a 22 AWG wire to one end of a coupon with silver epoxy. The coupon was then mounted in a chemically resistant acrylic compound to protect the exposed end of wire and the silver epoxy during the test and to provide an easily held sample (see figure 2 (a)). A single working electrode was placed in each test vessel. Glass sample holders were designed to hold the coupons at specific locations and orientations (see figure 2 (b)).

Two carbon graphite rods served as the counter electrodes. The rods were positioned in the cell to allow for a uniform current density to flow from the working electrodes (See Figure 4a). For these tests, an ORION™ saturated silver/silver chloride (SSC) electrode was utilized as the reference electrode. This electrode has shown excellent stability and reproducibility in previous high temperature testing. A PAR™ Model 273A Potentiostat/Galvanostat was used to conduct the tests. The software utilized for the PAR™ potentiostat was CorrWare™ for Windows.

For the tests performed in a dark environment, the same configuration that is shown in Figure 4a was set-up in a 1 liter glass beaker. The glass beaker was then placed inside a stainless steel beaker and covered with a Teflon™ cover (see Figure 4b). All openings to the vessel were carefully sealed to prevent exposure to light.

Test Matrix

The process variables that were explored in these studies are shown in Table 2. Four electrochemical tests were performed consecutively on a given sample. Initially, E_{corr} was monitored until a stable value was attained. Typically a stable value was obtained after 5 hours. After this time, the LPR test was conducted as described in ASTM standard G59 [6]. The scan rate that was used for these tests was 0.1 mV/s. The cathodic polarization test was performed next. The scan was initiated at E_{corr} and was ramped towards a potential 250 mV more negative than E_{corr} at a rate of 0.5 mV/s. The current density response was measured and a plot of potential vs. log current density was produced. Immediately following the cathodic polarization test, the anodic polarization test was performed [7]. The scan was initiated at 50 mV more negative than E_{corr} and then ramped towards a potential of 1.2 V vs. the Ag/AgCl reference electrode at a rate of 0.5 mV/s. As with the cathodic polarization study, a plot of potential vs. log current density was produced.

RESULTS

The results of the electrochemical tests are presented in this section. Table 3 shows the test number and the corresponding test conditions.

E_{corr} and Corrosion Rate Measurements

The results of the E_{corr} and corrosion rate measurements are summarized in Figure 3. The results of the tests were grouped into three categories of potentials for analysis. Group 1 results were characterized by high corrosion rates (> 50 mpy) and were the only tests where the potentials were in the range where hydrogen evolution was possible. The corrosion rates for Group 2 varied widely from less than 1 mpy to as high as 75 mpy. This indicates differences in the protective nature of the passive layer that was being formed. Group 3 on the other hand was characterized by noble potentials (~ > 150 mV) and low corrosion rates (< 20 mpy) indicative of a protective passive film. Specific effects of different process variables are discussed in the next section.

Anodic and Cathodic Behavior

Figure 4 shows examples of the types of anodic polarization curves that were observed during the electrochemical testing. Three regions were observed in general. The first region is between -400 mV to +200 mV and is a region of passivity (i.e., relatively low current density that is independent of potential), where the ferrous oxalate and oxide species are forming. The current responses of Test 3, 10 and 51A indicate that the process variables have a significant effect on the formation of the ferrous films. Note that the current density at +200 mV varies over a range of two orders of magnitude (i.e., the corrosion rate differs by as much as 2 orders of magnitude) among these three tests. As will be shown later in this section, the shape of the cathodic curve and the cathodic reactions occurring have a strong influence on the appearance of the anodic curve in this region.

In the potential range of +200 to +600 mV, the current was observed to increase significantly to a maximum. The maximum occurs between +400 to +600 mV and has been interpreted as representing the oxidation of ferrous ion to ferric ion. In this region the ferrous films are destroyed and result in a significant increase in the current.

At potentials greater than +600 mV, the region of constant current indicates the reformation of a passive iron oxide film. This film incorporates the ferric ion into its matrix. Although the current is fairly constant in this region, the current density is much higher indicating that this film is more porous than the ferrous film that was formed at the more negative potentials.

The anodic polarization scan for Test 34 shows a different type of behavior. In this case, no formation of the ferrous film was observed. The curve shows a constantly increasing current indicative of active dissolution of the ferrous film.

Specific effects of different process variables on the shape of these curves are discussed in the next section.

Figure 5 shows typical results from the cathodic polarization curve measurements. The initial slopes of the curves (i.e., the cathodic Tafel slope, Bc) and the magnitude of the currents observed indicate that the process variables had a significant effect on the cathodic behavior.

The following general observations on the cathodic curve behavior were made:

- The cathodic Tafel slope ranged from approximately 80 mV/decade at the more negative potential values to 140 mV/decade at the more positive potentials. These values indicate different cathodic reactions are active in these potential ranges. As indicated earlier, it is believed that the cathodic reaction at the more negative potentials involves hydrogen ion reduction, while at the more noble potentials, oxygen evolution or ferric ion reduction is more likely.
- The magnitude of the slopes were greater than the anodic Tafel slopes reported in oxalic acid solutions (i.e., 45 mV/decade [6]). This indicates that the corrosion reaction is more sensitive to changes in the reduction reaction kinetics than to changes in the oxidation kinetics (i.e., the corrosion reaction is cathodically controlled).
- As the E_{corr} became more positive, the curves indicated that the cathodic reaction was controlled more by diffusion processes. In Test 34 for example, as the potential is polarized from E_{corr}, the current density approaches a limiting value that is determined by the availability of the species involved in the cathodic reaction at the metal surface (i.e., concentration polarization). On the other hand, for Test 3 the current density appears to be constantly increasing indicating that the rate is limited by charge transfer at the metal surface (i.e., activation polarization).
- At similar values of E_{corr}, the cathodic curve can vary by one to two orders of magnitude (i.e., compare Test 51A and Test 34 in Figure 7 for example). Process variables such as agitation and temperature can significantly increase or reduce the availability of a species such as oxygen at the metal surface. Greater availability of oxygen would increase the rate of the cathodic reaction.

DISCUSSION

The effect of the environmental and material conditions on the corrosion behavior was examined. Table 3 shows the test number and the corresponding test conditions.

Eoc and Linear Polarization Tests

Table 4 summarizes the material and environmental conditions for each group. Although it was difficult to completely deconvolute the effects of the different variables the following general observations were made.

- The solution tested had a significant effect on the potential and corrosion rates. The presence of either sludge simulant in the oxalic acid shifted the potential in the more noble direction compared to the tests conducted in oxalic acid alone. The corrosion rates were generally higher in the oxalic acid solution than in the solutions that contained the sludge simulant with oxalic acid. Interestingly, Tank sludge simulant #1 was more aggressive than sludge stimulant #2 (i.e., higher corrosion rates). The color of sludge simulant #1 was lime green indicating the presence of the trisoxalatoiron (III) complex, whereas the color of sludge simulant #2 was a pale yellow. Thus, in sludge simulant #1 ferric ion reduction may be occurring, whereas another cathodic reaction such as oxygen reduction may be occurring sludge stimulant #2. This hypothesis was investigated further by the anodic and cathodic polarization tests.
- Temperature also had a strong influence on the observed corrosion rates and potentials. The E_{corr} for the 25°C tests was more positive than for tests at the other two temperatures. In general, the corrosion rates were also nearly an order of magnitude lower for the 25°C tests than for the other two temperatures. However, there were situations where the corrosion rate for the test performed at 75°C measured the same as the 25°C test and lower than the 50°C test.
- Coupons covered with the mill-scale or oxides were at more positive potentials and had lower corrosion rates than the polished coupons.
- The other variables (e.g., agitation, aeration, orientation, and light) did not have as strong of an effect as these first three. However, E_{corr} tended to be more positive for solutions that were agitated or aerated. The corrosion rates also appeared to be lower for the agitated and aerated solutions.

Anodic and Cathodic Tests

Tests 3 and 4 were compared to investigate the effect of adding sludge simulant #2 to oxalic acid. The other variables for the tests were the same: polished coupon, 50°C, aerated, agitated, light, and vertical orientation. Figure 6 illustrates the anodic behavior for these tests. Test 3, performed in oxalic acid only, exhibited passive behavior from E_{corr} up to +0.3 V where the ferrous film breaks down. On the other hand, Test 4 exhibits an active peak immediately after scanning anodically from E_{corr}. The current density exceeds that observed for the oxalic acid solution. This peak is indicative of a porous film at the metal surface initially. At approximately 0.0 V, the passive film appears to reform as an active to passive transition is observed. An active to passive transition was also observed between +0.4 to +0.5 V for both tests. In this case the film formed in the oxalic acid solution was more porous than that which was formed with the sludge slurry.

The cathodic polarization scans for Tests 3 and 4 are shown in Figure 7. The cathodic Tafel slope is significantly larger for Test 4 than Test 3. Evidently the presence of the other species in the sludge slurry changes the kinetics of the cathodic reaction. A slower cathodic reaction would in effect slow the rate of the anodic reaction (see Equation (9)) and hence the formation of the passive ferrous film. Therefore the peak current density in Figure 7, and the associated weaker passive film, can be understood.

Effect of Temperature

Tests 18A, 17A, and 16 were compared to investigate the difference in corrosion behavior in oxalic acid with sludge simulant #1 at 25, 50 and 75 °C, respectively. The other variables for the tests were the same: mill-scale coupon, aerated, agitated, light, and vertical orientation. Figure 8 illustrates the anodic behavior

for these tests. Both Tests 18A and 17A exhibit similar anodic behavior, although the test at the higher temperature (50°C) produced higher current densities indicative of less stable films. The curve for Test 16 (75°C) on the other hand initially had an active peak that produced high current densities followed by an active/passive transition at 0.15 V. The passive current density decreased to approximately the same value as that for Tests 18A and 17A. The higher peak current density at 0.4 V for Test 16 indicates that the film formed at 75°C was more porous than those formed at lower temperatures.

The cathodic polarization scans for Tests 18A (25°C), 17A (50°C), and 16 (75°C) are shown in Figure 9. The cathodic Tafel slopes for Tests 18A (25°C) and 16 (75°C) were unique. In both tests there appears to be two Tafel slopes. It is unclear whether this result was an experimental artifact or there is a transition from one cathodic reaction to another. Either way, the cathodic Tafel slopes measured for Test 18A are less than those for Test 16. For example, if the Tafel slope is obtained assuming that the "hump" does not exist, the values for both Tests18A and 16 are approximately 50 and 100 mV/decade, respectively. The other interesting facet of these curves is that the effect of concentration polarization is greater for Test 18A. Both of these observations suggest that different cathodic reactions are occurring at the different temperatures. At 25°C, the solubility oxygen is much greater in the solution than it is at 75°C. On the other hand, at 75°C, the solubility of the ferric ion is much greater than it is at 25°C. Therefore it is concluded that in the dissolved sludge solutions that oxygen reduction is the favored cathodic reaction at low temperatures, while ferric ion reduction is the more favored reaction at the higher temperatures. If this is true, aeration should have a significant effect on the polarization tests performed at 25°C should be observed, while little or no effect would be expected at 75°C.

Effect of Surface Conditions

Four different surface conditions were examined during the testing. Comparisons of the anodic and cathodic polarization scans were made between mill-scale and polished, and the mill-scale and mill-scale with oxide coupons. Tests 49 and 51A were compared to investigate the difference in corrosion behavior between mill-scale and polished coupon surfaces, respectively. The other variables for these tests were identical: oxalic acid and sludge stimulant #1, 50°C, aerated, agitation, dark, and vertical orientation. Figure 10 illustrates the anodic behavior for these tests. The shapes of the curves were similar, although the current density at a given potential was greater for the polished coupon up until the breakdown of the mill-scale. The breakdown of the ferrous film on the polished specimen (Test 51A) began at a potential approximately 100 mV more positive than the breakdown potential for the mill-scale coupon. This indicates that although the mill-scale is more protective initially, it is more susceptible to breakdown than the film that is formed by ferrous oxalate and ferrous oxide.

The cathodic polarization scans for Tests 49 and 51A are shown in Figure 11. The cathodic Tafel slope for the mill-scale sample (106 mV/decade) was less than that for the polished sample (140 mV/decade) indicating faster reduction kinetics on the mill scale coupon. One possible explanation for this observation is that the mill-scale on the coupon that was utilized for the Test 49 surface was not coherent (i.e., there were breaks in the film exposing bare metal), and hence the reduction kinetics were facilitated. The ferrous oxide/ferrous oxalate film that formed on the coupon in Test 51A on the other hand was more consistent, even though it may have been more porous.

Effect of Aeration

Tests 18A and 41 were compared to investigate the difference in corrosion behavior for an aerated and de-aerated oxalic acid with sludge simulant, respectively at the low temperature (i.e., 25°C). Sludge simulant #2 was used for Test 41, while Test 18A utilized sludge simulant #1. Additionally Test 41 was not agitated, while agitation was utilized for Test 18A. This would function to increase the velocity of the solution at the metal surface and therefore reduce the effects of concentration polarization particularly oxygen. The other variables for the tests were identical: mill-scale coupon, light, and vertical orientation. Figure 12 illustrates the anodic behavior for these tests. The de-aerated solution demonstrated active dissolution and initiated from a more positive E_{corr} potential than the aerated case. The aerated test on the other hand demonstrated a small degree of passive behavior followed by breakdown of the ferrous film. This result indicates that the presence of oxygen has a significant effect at the lower temperatures. The

higher current densities for Test 18A than Test 41 are likely reflective of the degree of agitation and differences in the sludge simulant.

The cathodic polarization scans for Tests 18A and 41 are shown in Figure 13. The cathodic Tafel slope for the de-aerated solution (0.135 V/decade) was greater than the slope for the aerated solution (0.053 V/decade). The de-aerated curve also showed more evidence of concentration polarization as the potential became more negative. Both the greater slope and the evidence of concentration polarization observed for Test 41 also suggest that agitation for had a significant effect on these two tests. The significant shift in E_{corr} to a more positive potential in the de-aerated, indicates that the ferric ion is the likely cathodic reaction in the de-aerated solution. On the other hand, the aeration and agitation result in more oxygen available at the metal surface for Test 18A.

Effect of Agitation

Agitation increases the velocity of the solution near the metal surface and therefore is expected to reduce the effects of concentration polarization. Both the ferric ion and oxygen reduction reactions have exhibited concentration polarization effects. Two comparisons examined the effects of agitation. Tests 36A and 37A compares the difference in corrosion behavior for an agitated and non-agitated oxalic acid with sludge simulant #1, respectively. The other variables for the tests were identical: mill-scale coupon, 75°C, aerated, light, and vertical orientation. Figure 14 illustrates the anodic behavior for these tests. The shapes of the curves were very similar (i.e., initial active/passive behavior followed by breakdown of the ferrous film). The current density at the current peak at +150 mV was higher for the agitated solution during the formation of the ferrous film; however, they were similar for the formation of the ferric film. The increase in the velocity may have increased the availability of the hydrogen-oxalate ion at the surface and thus increased the rate of formation of the ferrous films as reflected by the higher current density for Test 36A.

The cathodic polarization scans for Tests 36A and 37A are shown in Figure 15. As indicated in previous tests at 75°C, the cathodic reaction is ferric ion reduction. The cathodic Tafel slope for the non-agitated solution was 0.098 V/decade. Although the data quality for Test 36A is not as good, it appears that the cathodic current density is slightly higher. Thus, agitation reduced the concentration polarization behavior of the ferric ion reduction reaction and results in a higher corrosion rate.

Effect of Orientation

Observations of coupon tests indicated that the ferrous oxalate deposits on horizontally oriented coupons are significantly thicker than those observed on vertical coupons [1]. These thick deposits are expected to hinder the corrosion reaction. Tests 16 and 24 investigated the difference in corrosion behavior for vertically and horizontally oriented coupons, respectively, in an oxalic acid with sludge simulant #1, respectively. The other variables for the tests were identical: mill-scale coupon, 75°C, aerated, and light. Figure 16 illustrates the anodic behavior for these tests. The shapes of the curves were similar (i.e., initial passive behavior followed by breakdown of the ferrous film). The current density was significantly lower for the horizontally oriented coupon compared with the vertically oriented coupon at all potentials up to the formation of the ferric films. This behavior is indicative of a more protective ferrous film on the surface of the coupon.

The cathodic polarization scans for Tests 16 (vertical) and 24 (horizontal) are shown in Figure 17. As indicated in previous tests at 75°C, the cathodic reaction is ferric ion reduction. The cathodic Tafel slope for the vertically oriented coupon was 0.098 V/decade, while for the horizontally oriented coupon was slightly higher measuring 0.104 V/decade. The orientation did not seem to have a significant influence on the reduction kinetics. It is believed that the difference in corrosion rates for the two orientations is a function of the thickness of the deposited film.

CONCLUSION

Electrochemical testing was performed to investigate the corrosion behavior of carbon steel exposed to the oxalic acid chemical cleaning solution. The significant results of the study were the following.

1) The dominant cathodic reaction was hydrogen evolution in tests in oxalic acid solutions on polished coupons.
2) The addition of sludge simulant to the test changed the active cathodic reaction from hydrogen evolution to either oxygen reduction or ferric ion reduction.
3) The ferric ion reduction reaction was dominant in high temperature solutions (50°C and 75°C) where oxygen solubility was low and ferric ion solubility was high.
4) The oxygen reduction reaction was dominant at the low temperature (25°C) where oxygen solubility was high and ferric ion solubility was low.
5) De-aerated conditions favor either the ferric ion reduction or hydrogen evolution cathodic reactions.
6) Agitation reduces the degree of concentration polarization. The rate of ferric ion reduction and oxygen reduction both increased with agitation, while the rate of the hydrogen evolution reaction did not change significantly.
7) The mill scale surface protects the surface from attack initially. However, the mill scale breaks down more quickly than the ferrous films formed by the corrosion process.
8) The corrosion rates were the highest when the hydrogen evolution reaction was dominant.
9) The corrosion rates were higher when the cathodic reaction involved the ferric ion rather than oxygen.
10) The thick ferrous films that form on horizontally oriented surfaces are more stable and hence more protective than the films that form on the vertical surfaces. The orientation of the surface did not influence the cathodic reaction significantly.
11) The ferrous films that form in a light environment are more stable and hence more protective than the films that form in a dark environment. Light did not influence the cathodic reaction.

REFERENCES

1) H. H. Uhlig, Corrosion and Corrosion Control, 2nd Edition, John Wiley and Sons, NY, NY, 1971.
2) S. N. Saltykov, "A Mechanism of the Anodic Dissolution of Armco Iron and High Strength Ferritic Cast Iron in an Oxalate Medium", Protection of Metals, Vol. 37, No. 2, pp. 186-191, 2001.
3) M. A. Streicher, "Synergistic Inhibition of Ferric Ion Corrosion During Chemical Cleaning of Metal Surfaces", Corrosion, Vol. 28, No. 4, p. 143, April, 1972.
4) H. D. Smith, R. L. Russell, and G. K. Patello, "Evaluation of Hydrogen Gas Generation from Oxalic Acid Contact with the Carbon Steel of a High Level Waste Storage Tank," In Environmental Issues and Waste Management Technologies in the Ceramic and Nuclear Industries, Eds. J. C. Marra and G. T. Chandler, Ceramic Transactions, Vol. 93, pp. 221-227, 1999.
5) M. R. Elmore, "Corrosion of Mild Steel in Simulated Cesium Elution Process Solutions", PNNL-11284, September, 1996.
6) "Standard Test Method for Conducting Potentiodynamic Polarization Resistance Measurements," ASTM G59-97, Reapproved in 2003.
7) "Standard Reference Test Method for Making Potentiostatic and Potentiodynamic Anodic Polarization Measurements," ASTM G5-94, Reapproved in 2004.

Table 1. The material is ASTM A537 Class I carbon steel. The compositions shown are in wt%

Al	C	Cr	Cu	Mn	Mo	Ni	P	S	Si	Fe
0.066	0.18	0.16	0.157	1.31	0.055	0.18	0.018	0.01	0.279	balance

Table 2. Test Variables for Electrochemical Studies.

Variable	Parameters
Temperature	25, 50 and 75 °C
Oxygen	De-aerated (with nitrogen) and Aerated
Surface Condition	Polished, Polished with Iron Oxide, Mill Scale, and Mill-scale with iron oxide
Orientation	Horizontal and Vertical
Agitation	None and Mixing with a magnetic stir bar
Solution Composition	8 wt.% Oxalic Acid and 8 wt.% Oxalic Acid with Sludge and Supernate Simulant (the ratio of oxalic acid to sludge simulant was 20:1 by volume); Two sludge simulants were tested
Photocatalytic Activity	Dark and Light

Table 3. Matrix showing test number and corresponding conditions. OA is Oxalic Acid; Yellow highlight indicates sludge stimulant #2 was utilized. In all other cases, the sludge stimulant #1 was utilized.

Test #	Surface Finish				Solution		Temperature			Agitation	Orientation	Light	Aerated
	Mill Scale	Mill Scale + w/oxide	Polished	Polished w/oxide	OA	OA+Sludge	25 C	50 C	75 C				
1			x		x			x		x	Vertical	x	x
2			x			x		x		x	Vertical	x	x
3			x		x			x			Vertical	x	x
4			x			x		x			Vertical	x	x
5			x		x			x			Vertical	x	
6			x			x		x			Vertical	x	
7			x		x			x			Vertical	x	
8			x			x		x			Vertical	x	
9			x		x			x			Vertical	x	x
10			x			x		x			Vertical	x	x
11			x		x				x		Vertical	x	x
12			x			x			x		Vertical	x	x
13			x		x				x		Vertical	x	
14			x			x			x		Vertical	x	
15	x					x	x				Vertical	x	x
15A	x					x	x				Vertical	x	x
16	x					x			x	x	Vertical	x	x
17	x					x		x		x	Vertical	x	x
18	x					x	x			x	Vertical	x	x
18A	x					x	x			x	Vertical	x	x
19	x					x			x		Vertical	x	x
20	x					x	x			x	Vertical		x
Test #	Surface Finish				Solution		Temperature			Agitation	Orientation	Light	Aerated
	Mill Scale	Mill Scale + w/oxide	Polished	Polished w/oxide	OA	OA+Sludge	25 C	50 C	75 C				
21	x					x	x				Vertical	x	x
22	x					x			x	x	Vertical	x	x
23	x					x			x	x	Horizontal	x	x
24	x					x			x		Horizontal	x	x
25	x					x		x		x	Horizontal	x	x
25A	x					x		x		x	Horizontal	x	x
26	x					x		x			Horizontal	x	x
27	x					x	x			x	Horizontal	x	x
28	x					x	x				Horizontal	x	x
28A	x					x	x				Horizontal	x	x
29		x				x		x		x	Vertical	x	x
29A		x				x		x		x	Vertical	x	x
30		x				x		x			Vertical	x	x
31				x		x		x		x	Vertical	x	x
32				x		x		x			Vertical	x	x
33	x					x	x				Vertical	x	x
34		x				x	x				Vertical	x	x
35			x			x	x				Vertical	x	x
36	x					x			x	x	Vertical	x	
36A	x					x			x	x	Vertical	x	
37	x					x			x		Vertical	x	
37A	x					x			x		Vertical	x	
37B	x					x			x		Vertical	x	
38	x					x		x		x	Vertical	x	
38A	x					x		x		x	Vertical	x	
39	x					x		x			Vertical	x	
39A	x					x		x			Vertical	x	
Test #	Surface Finish				Solution		Temperature			Agitation	Orientation	Light	Aerated
	Mill Scale	Mill Scale + w/oxide	Polished	Polished w/oxide	OA	OA+Sludge	25 C	50 C	75 C				
40	x					x	x			x	Vertical	x	
41	x					x	x				Vertical	x	
42		x				x			x	x	Vertical	x	
43		x				x			x		Vertical	x	x
43A		x				x			x		Vertical	x	x
44		x				x		x		x	Vertical	x	
45		x				x		x			Vertical	x	x
46		x				x	x			x	Vertical	x	
47		x				x	x				Vertical	x	x
48	x					x			x	x	Vertical		x
49	x					x		x		x	Vertical		x
50			x		x			x		x	Vertical		x
51			x			x		x		x	Vertical		x
51A			x			x		x		x	Vertical		x
52			x		x			x			Vertical		x
52A			x		x			x			Vertical		x
53			x			x		x			Vertical		x
53A			x			x		x			Vertical		x
54	x					x			x		Vertical		x
55	x					x		x			Vertical		x
56	x					x	x				Vertical		x
57	x					x		x			Vertical	x	x

Table 4. Summary of the Material and Environmental Conditions within each Group.

Group	Material and Environmental Conditions
1 (corrosion rate 50 - 200 mpy)	Polished coupons; solution was oxalic acid; temperatures were 50 to 75°C; with and without agitation; aerated and de-aerated; light and dark environment. Two low corrosion rates in this group occurred when Tank 8 sludge slurry was added to the oxalic acid solution. The E_{corr} values were also higher for these two tests.
2 (corrosion rates 20-75 mpy)	Mill-scale, Mill-scale with oxide and Polished with oxide coupons; Solution was oxalic acid with sludge stimulant #1; temperatures were 50 to 75°C; with and without agitation; aerated and de-aerated; light and dark environment.
2 (corrosion rates < 20 mpy)	Polished, Mill-scale, Mill-scale with oxide coupons, oxalic acid with both sludge simulants, temperatures were 25, 50, and 75°C; with and without agitation; aerated and de-aerated; light and dark environment. Higher corrosion rates within this region were observed in sludge stimulant #1 than in sludge stimulant #2 at the higher temperatures.
3 (corrosion rates < 20 mpy)	Mill-scale and Mill-scale with oxide coupons, oxalic acid with either sludge simulant, temperatures were 25, 50, and 75°C; with and without agitation; aerated and de-aerated; light and dark environment; horizontal orientation.

(a) (b)

Figure 1. Examples of surface finish on working electrode: a) polished coupon, and b) mill-scale coupon.

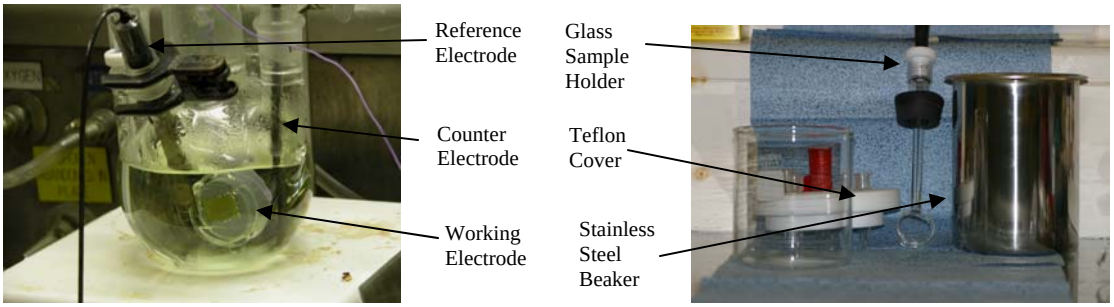

(a) (b)

Figure 2. Test cell for a) Lighted Environment, and b) Dark Environment

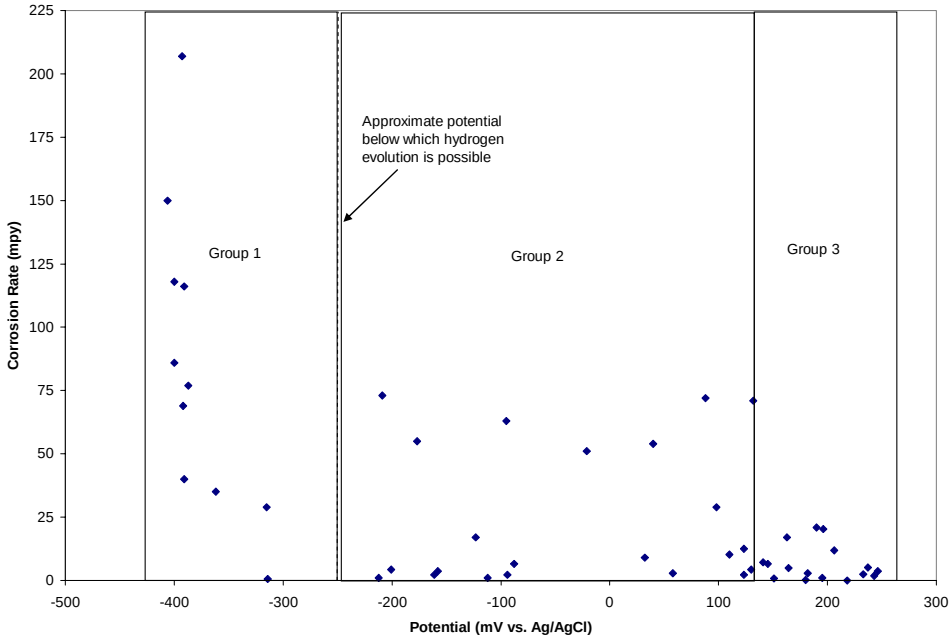

Figure 3. Distribution of E_{corr} and corrosion rates for the electrochemical tests.

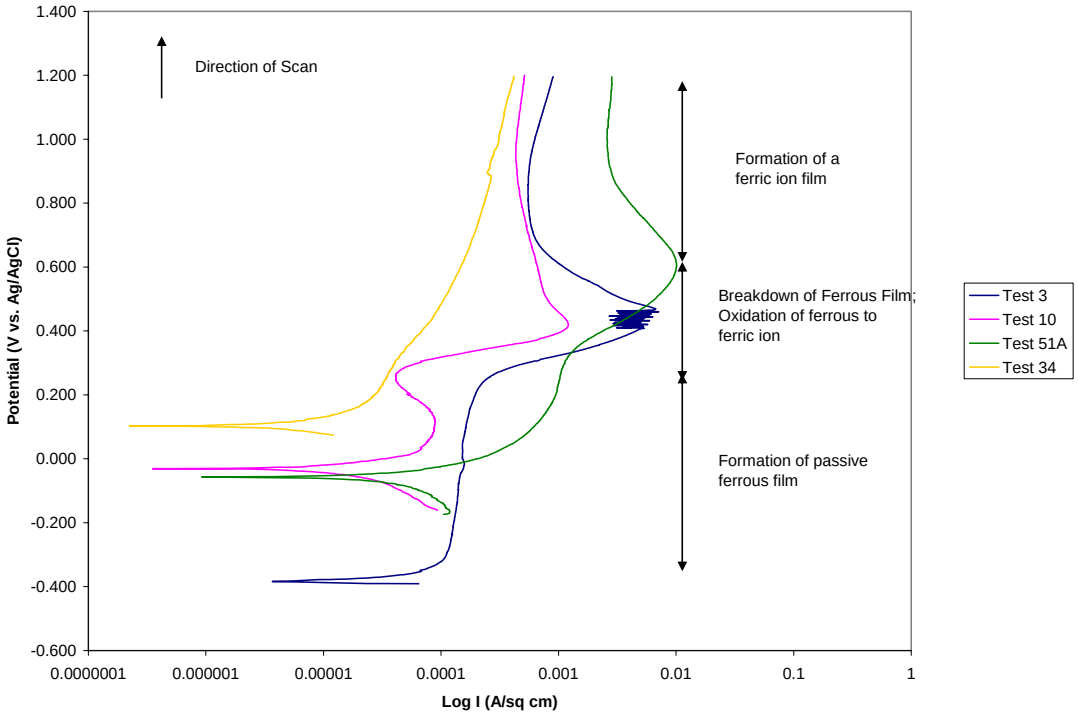

Figure 4. General behavior for the anodic polarization curves. Results from Tests 3, 10, 51A, and 34 are shown as examples.

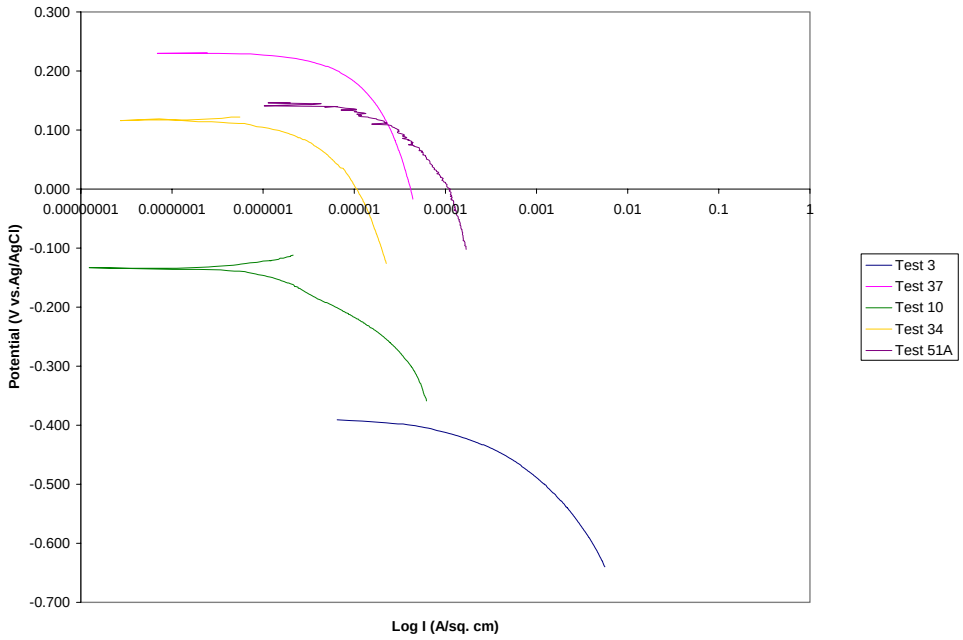

Figure 5. General behavior for the cathodic polarization curves. Results from Tests 3, 37, 10, 34, and 51A are shown as examples.

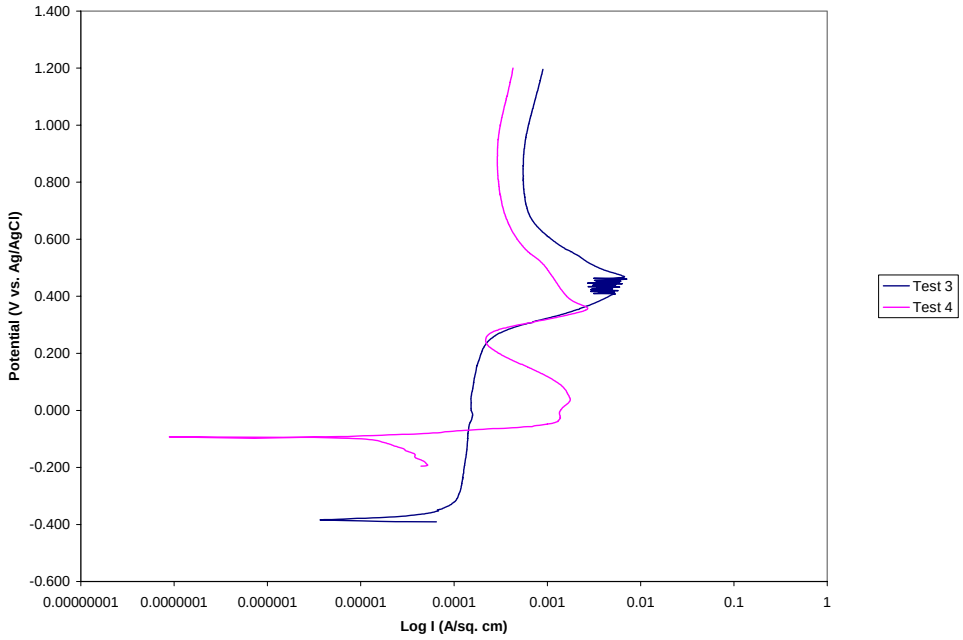

Figure 6. Effect of solution tested: OA vs. Sludge Simulant #2. Anodic behavior during Tests 3 and 4.

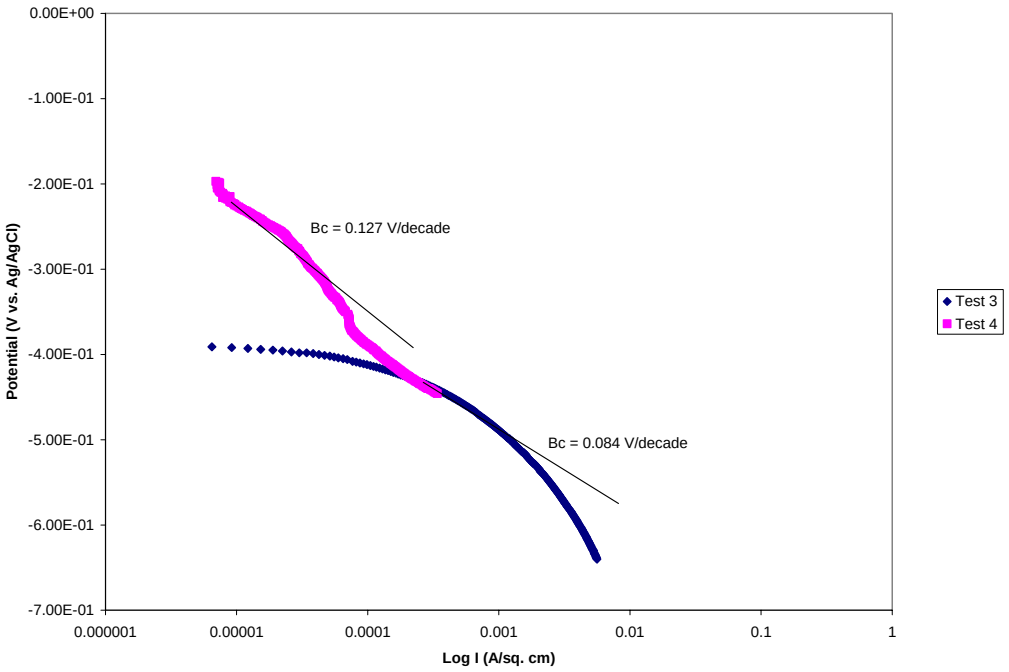

Figure 7. Effect of solution tested: OA vs. Sludge Simulant #2. Cathodic behavior during Tests 3 and 4.

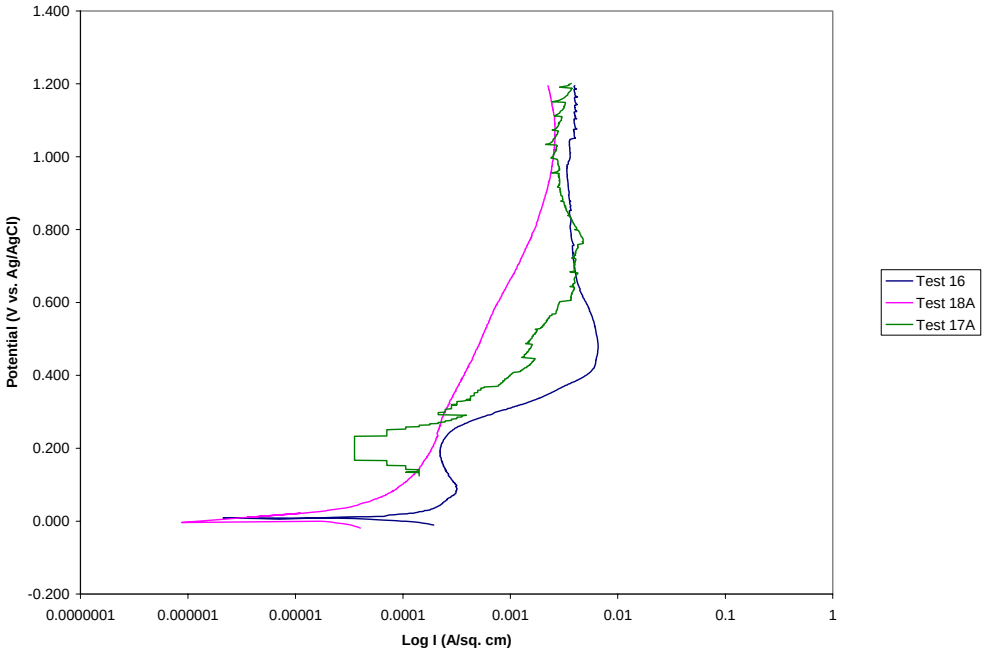

Figure 8. Effect of temperature tested in Sludge stimulant #1: Anodic behavior for Tests 18A (25°C), 17A (50°C), and 16 (75°C).

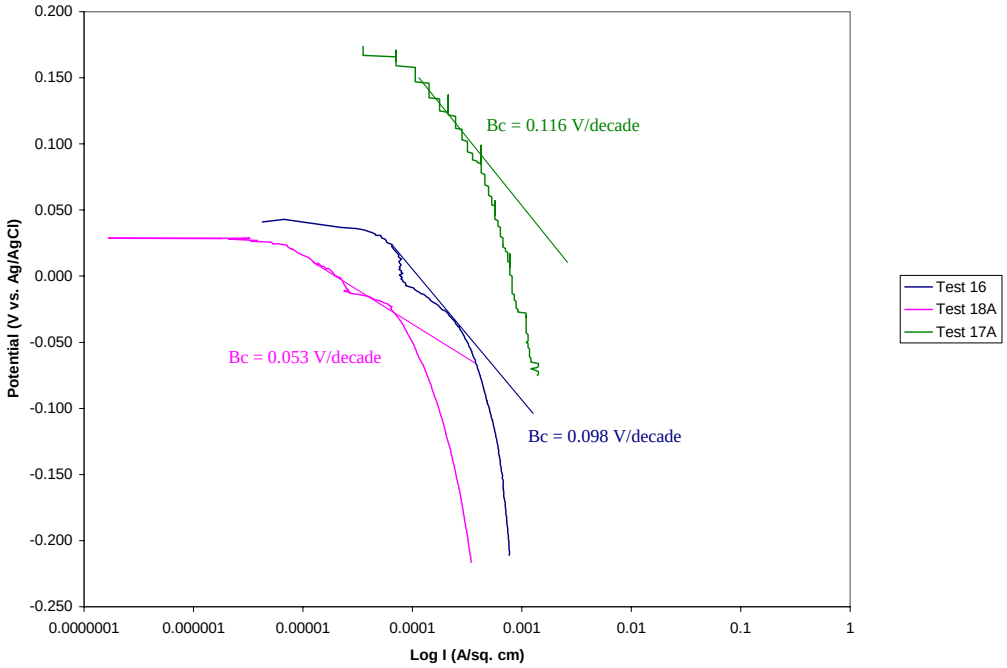

Figure 9. Effect of temperature tested in Sludge Simulant #1: Cathodic behavior for Tests 18A (25°C), 17A (50°C), and 16 (75°C)

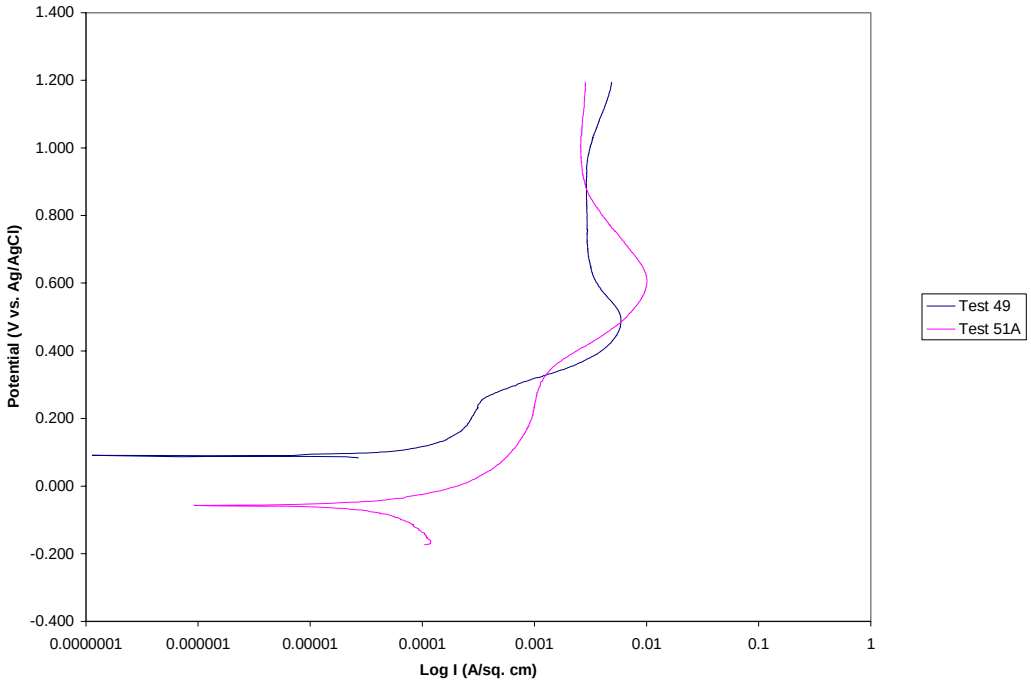

Figure 10. Effect of mill scale vs. polished surface: Anodic behavior for Tests 49 (mill-scale) and 51A (polished).

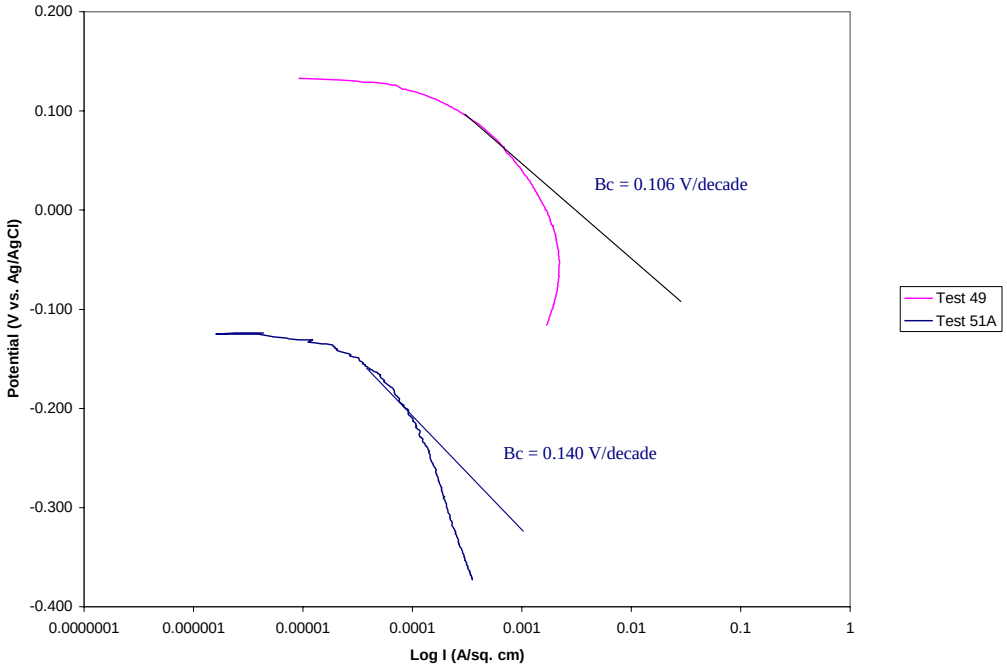

Figure 11. Effect of mill scale vs. polished surface: Cathodic behavior for Tests 49 (mill-scale) and 51A (polished).

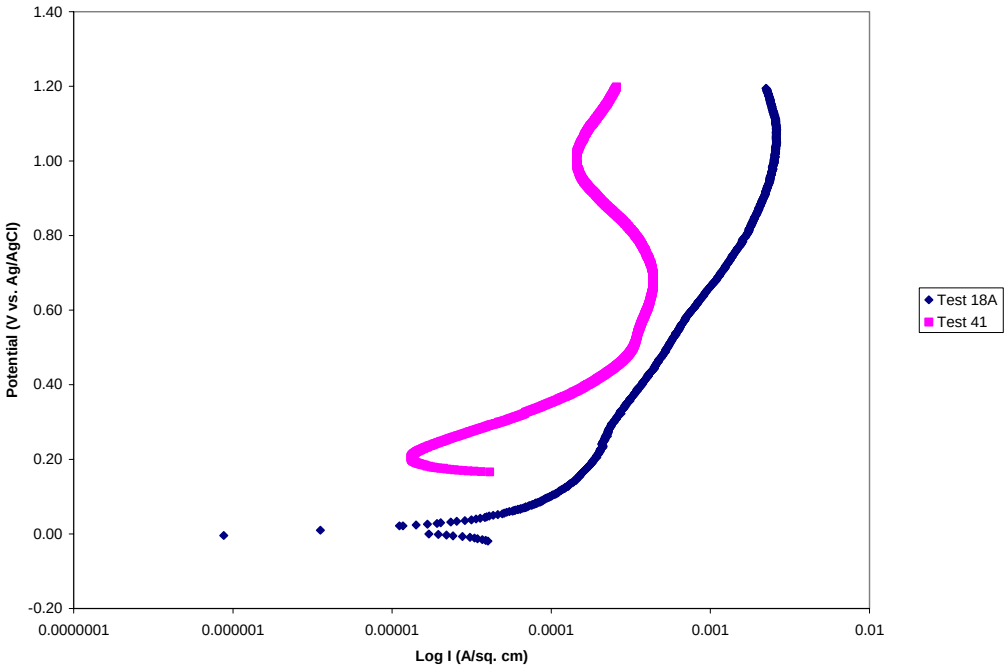

Figure 12. Effect of Aeration in sludge simulant solution at Low Temperature: Anodic behavior for Tests 18A (aerated) and 41 (de-aerated).

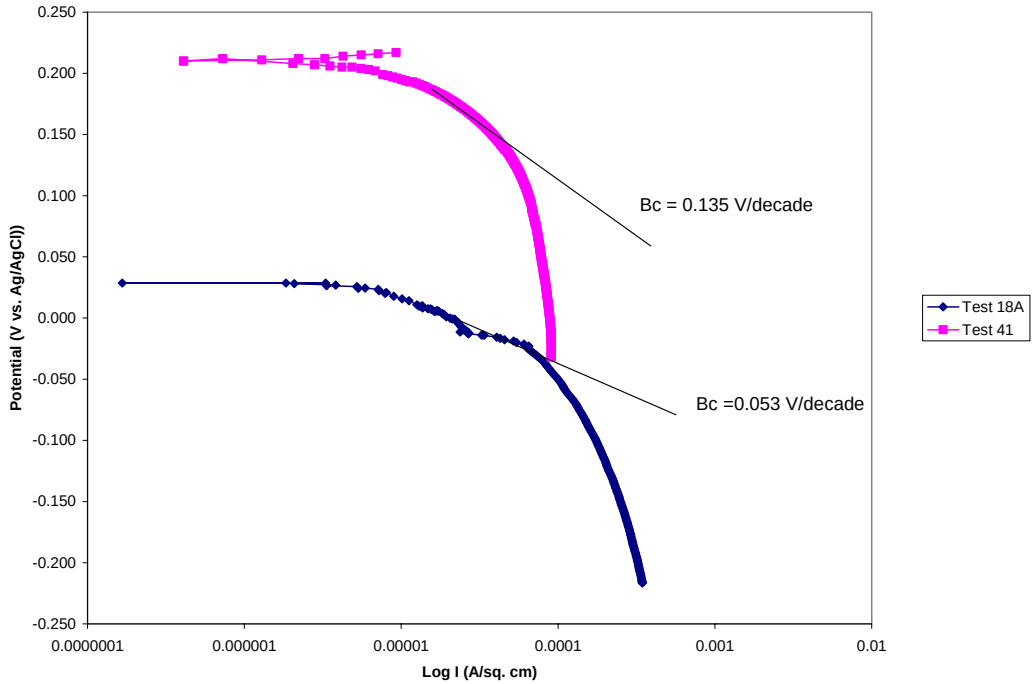

Figure 13. Effect of Aeration in sludge simulant at Low Temperature: Cathodic behavior for Tests 18A (aerated) and 41 (de-aerated).

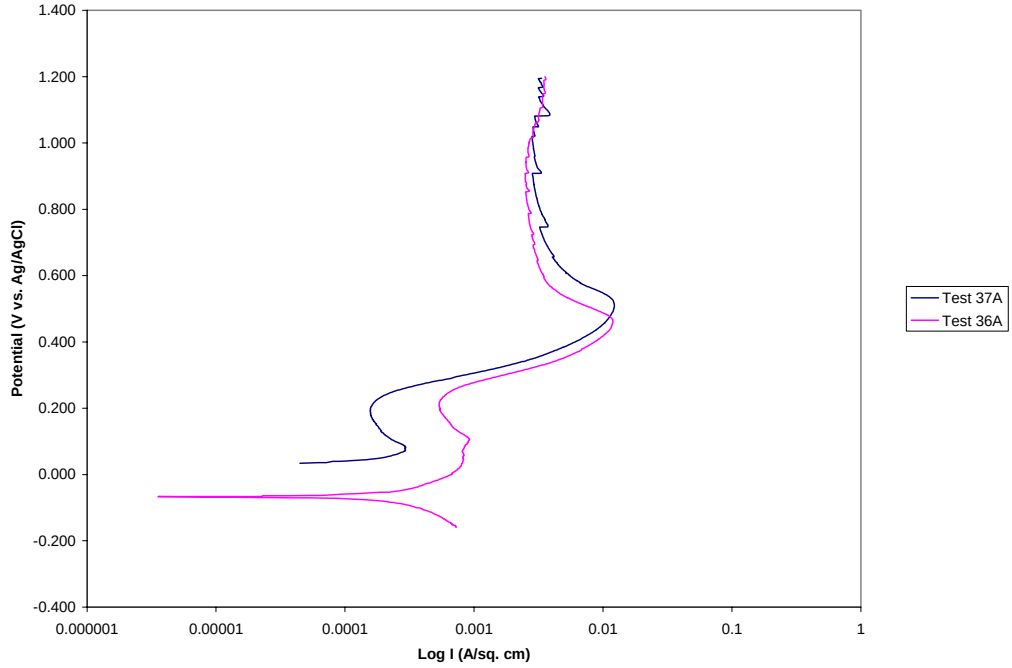

Figure 14. Effect of Agitation in sludge simulant #1: Anodic behavior for Tests 36A (agitated) and 37A (not agitated).

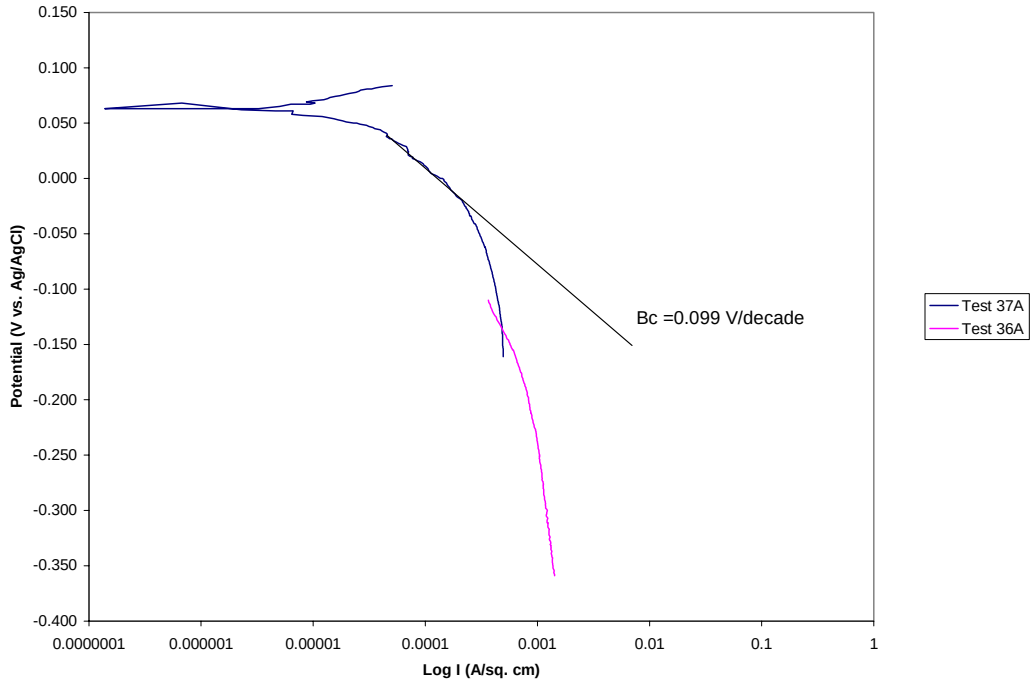

Figure 15. Effect of Agitation in sludge simulant #1: Cathodic behavior for Tests 36A (agitated) and 37A (not agitated).

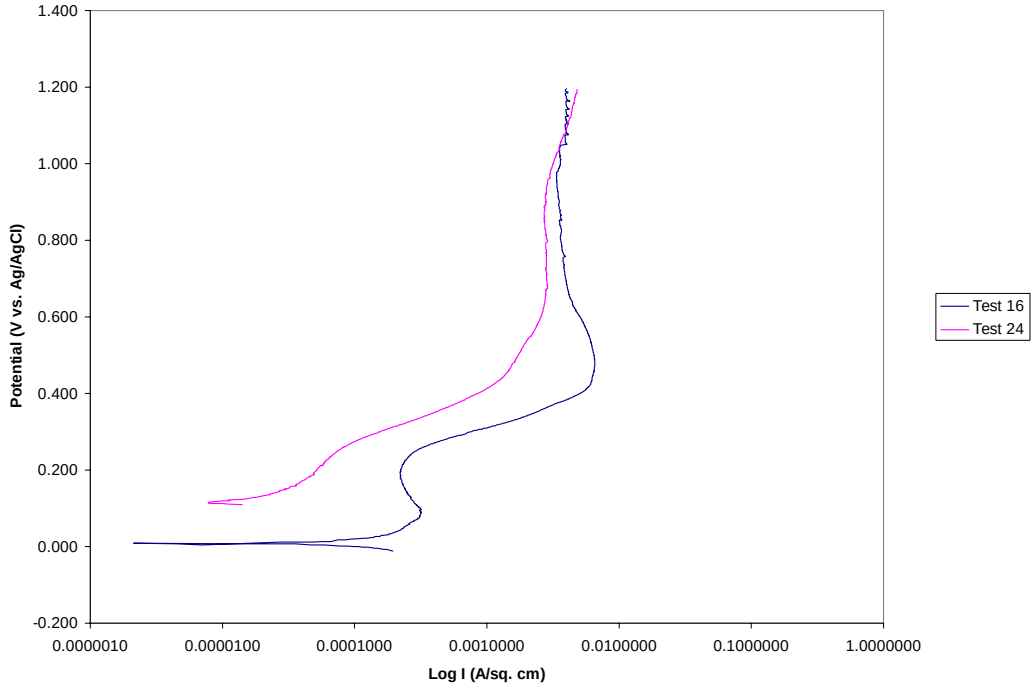

Figure 16. Effect of Horizontal vs. Vertical orientation: Anodic behavior for Tests 16 (vertical) and 24 (horizontal).

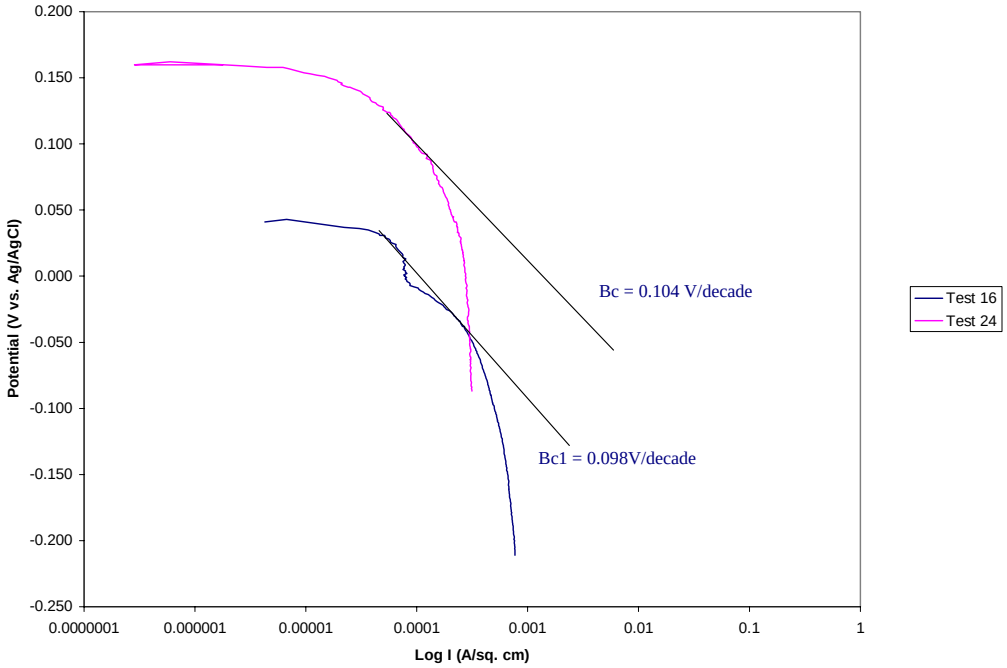

Figure 17. Effect of Horizontal vs. Vertical orientation: Cathodic for Tests 16 (vertical) and 24 (horizontal).